**Article details**

Yamamoto Y., Välitalo P.A., Wong Y.C., Huntjens D.R., Proost J.H., Vermeulen A., Krauwinkel W., Beukers M.W., Kokki H., Kokki M., Danhof M., Hasselt J.G.C. van & Lange E.C.M. de (2018), Prediction of human CNS pharmacokinetics using a physiologically-based pharmacokinetic modeling approach, E*uropean Journal of Pharmaceutical Sciences* 112: 168-179.
Doi: 10.1016/j.ejps.2017.11.011

European Journal of Pharmaceutical Sciences 112 (2018) 168–179

Contents lists available at ScienceDirect

European Journal of Pharmaceutical Sciences

journal homepage: www.elsevier.com/locate/ejps

# Prediction of human CNS pharmacokinetics using a physiologically-based pharmacokinetic modeling approach

Yumi Yamamoto[a], Pyry A. Välitalo[a], Yin Cheong Wong[a], Dymphy R. Huntjens[b], Johannes H. Proost[c], An Vermeulen[b], Walter Krauwinkel[d], Margot W. Beukers[e], Hannu Kokki[f,g], Merja Kokki[f,g], Meindert Danhof[a], Johan G.C. van Hasselt[a], Elizabeth C.M. de Lange[a,*]

[a] Division of Pharmacology, Cluster Systems Pharmacology, Leiden Academic Centre for Drug Research, Leiden University, Leiden, The Netherlands
[b] Quantitative Sciences, Janssen Research & Development, a division of Janssen Pharmaceutica NV, Beerse, Belgium
[c] Division of Pharmacokinetics, Toxicology and Targeting, University of Groningen, Groningen, The Netherlands
[d] Department of Clinical Pharmacology & Exploratory Development, Astellas Pharma BV, Leiden, The Netherlands
[e] Science Business Support, Leiden, The Netherlands
[f] Department of Anesthesia and Operative Services, Kuopio University Hospital, Kuopio, Finland
[g] School of Medicine, University of Eastern Finland, Kuopio, Finland

ARTICLE INFO

*Keywords:*
Physiology-based pharmacokinetics (PBPK)
Blood-brain barrier
Translational modeling
Disease effects
CNS
Active transport

ABSTRACT

Knowledge of drug concentration-time profiles at the central nervous system (CNS) target-site is critically important for rational development of CNS targeted drugs. Our aim was to translate a recently published comprehensive CNS physiologically-based pharmacokinetic (PBPK) model from rat to human, and to predict drug concentration-time profiles in multiple CNS compartments on available human data of four drugs (acetaminophen, oxycodone, morphine and phenytoin).

Values of the system-specific parameters in the rat CNS PBPK model were replaced by corresponding human values. The contribution of active transporters for the four selected drugs was scaled based on differences in expression of the pertinent transporters in both species. Model predictions were evaluated with available pharmacokinetic (PK) data in human brain extracellular fluid and/or cerebrospinal fluid, obtained under physiologically healthy CNS conditions (acetaminophen, oxycodone, and morphine) and under pathophysiological CNS conditions where CNS physiology could be affected (acetaminophen, morphine and phenytoin).

The human CNS PBPK model could successfully predict their concentration-time profiles in multiple human CNS compartments in physiological CNS conditions within a 1.6-fold error. Furthermore, the model allowed investigation of the potential underlying mechanisms that can explain differences in CNS PK associated with pathophysiological changes. This analysis supports the relevance of the developed model to allow more effective selection of CNS drug candidates since it enables the prediction of CNS target-site concentrations in humans, which are essential for drug development and patient treatment.

## 1. Introduction

Development of drugs for central nervous system (CNS) diseases faces high attrition rates (Arrowsmith and Miller, 2013). A major factor for this high attrition rate is the lack of adequate information on unbound drug concentration-time profile at the CNS target-sites, which is the driving force for the drug-target interaction and subsequent drug effect (Danhof et al., 2007).

Several factors govern the distribution of drug molecules into and within the CNS. Physiological CNS compartments include the brain microvascular (brainMV) space, the key drug-target site compartments being the brain extracellular fluid ($brain_{ECF}$), the brain intracellular fluid ($brain_{ICF}$), and also multiple cerebrospinal fluid (CSF) spaces. CNS drug distribution is governed by several processes including physiological fluid flows, passive and active membrane transport across the blood–brain barrier (BBB) and the blood–CSF barrier (BCSFB), extracellular-intracellular exchange, and pH differences (Westerhout et al., 2011). Physiological fluid flows include cerebral blood flow (CBF), $brain_{ECF}$ bulk flow, and CSF flow. The interplay between various processes complicates prediction of drug target-site concentrations. In addition, aging and pathophysiological conditions may alter CNS drug distribution. This happens for example *via* changes in properties of the

* Corresponding author at: Leiden University, Gorlaeus Laboratories, Einsteinweg 55, 2333CC, The Netherlands.
*E-mail address:* ecmdelange@lacdr.leidenuniv.nl (E.C.M. de Lange).

https://doi.org/10.1016/j.ejps.2017.11.011
Received 7 September 2017; Received in revised form 7 November 2017; Accepted 10 November 2017
Available online 11 November 2017
0928-0987/ 

BBB and BCSFB (*e.g.* opening of tight junctions, decrease in some tight junction proteins, increase/decrease of the expression level of active transporters), volumes of CNS compartments and CNS fluid flows (Deo et al., 2013; Yamamoto et al., 2017a), and should therefore be taken into account in CNS pharmacokinetic (PK) predictions.

To investigate CNS drug distribution, *ex vivo* techniques such as the brain homogenate and the brain slicing technique are currently used. With these techniques, steady state values of the unbound fraction in brain (Kalvass and Maurer, 2002) and the volume of distribution of the unbound drug in brain (Friden et al., 2007) can be determined, from which also intracellular accumulation of the unbound drug can be derived. Unfortunately, these techniques cannot provide information on the unbound drug concentration-time profiles, and potential local concentration differences. Such information is very important for determining the rate and extent of processes in CNS drug distribution and understanding their interrelationships (systems pharmacokinetics). Time course data of unbound drug concentrations can only be obtained by *in vivo* intracerebral microdialysis (de Lange et al., 1994; Westerhout et al., 2012, 2013, 2014), as other monitoring techniques like positron emission tomography measure total drug concentrations (Dresel et al., 1998; Mamo et al., 2004; Neuwelt et al., 2008). However, though minimally invasive, the use of microdialysis in humans is highly restricted. Therefore, approaches that can predict time-dependent and CNS location-dependent unbound drug concentration in human are of great interest.

We recently developed a comprehensive physiologically-based pharmacokinetic (PBPK) rat model to predict unbound drug concentration-time profiles for multiple CNS compartments (Yamamoto et al., 2017b). This rat PBPK model allows prediction of CNS PK profiles without the need of *in vivo* PK data. The purpose of the present study was to scale the rat CNS PBPK model to predict drug PK profiles in multiple CNS compartments in human. The human CNS PBPK model was evaluated using available human $brain_{ECF}$ and/or CSF PK data. Since measurement of the drug concentration in human CNS is highly limited due to ethical and practical constraints, PK data from four compounds such as acetaminophen, oxycodone, morphine, and phenytoin in physiological and/or pathophysiological CNS conditions, were used in this analysis.

## 2. Materials and methods

The previously developed rat CNS PBPK model (Yamamoto et al., 2017b), which consisted of a plasma PK and a CNS PBPK component, was scaled to predict human CNS PK by substitution of rat CNS physiological parameter values by the human values (Fig. 1). Human plasma PK models for the drugs investigated (acetaminophen, oxycodone, morphine, phenytoin) were either obtained from literature or developed using available human plasma data.

All analyses were performed using NONMEM version 7.3 (Beal et al., 2010). The predictive performance of the developed model was evaluated using available human data on the concentrations of acetaminophen, oxycodone, morphine and phenytoin in $brain_{ECF}$ and/or CSF, obtained under physiological and/or pathophysiological CNS conditions.

### 2.1. Human plasma and CNS data

The details of the clinical PK studies of acetaminophen, oxycodone, morphine and phenytoin, which were used for the evaluation of the human PBPK model predictions, are summarized in Table 1.

#### 2.1.1. Acetaminophen

Human acetaminophen PK data in plasma and in CSF in the lumbar region ($CSF_{SAS\_LUMBAR}$) were obtained from healthy subjects (study A1) and from patients with nerve-root compression pain (study A2) (Bannwarth et al., 1992; Singla et al., 2012). These CNS conditions were considered to be physiological CNS conditions, *i.e.* without likely effects on CNS PK. In study A3, human CSF samples from the lateral ventricle ($CSF_{LV}$) were obtained by extra-ventricular drainage (EVD) ($CSF_{EVD}$) from patients with traumatic brain injury (TBI), which was considered as a pathophysiological CNS condition (Yamamoto et al., 2017c). For all datasets, total plasma concentrations for acetaminophen were converted to unbound plasma concentrations using the free fraction (85%) obtained from literature for healthy subjects (Gazzard et al., 1973).

#### 2.1.2. Oxycodone

Oxycodone human plasma and $CSF_{SAS\_LUMBAR}$ PK data (study O1) were obtained from patients under elective gynecological surgery (Kokki et al., 2014), where a CNS condition considered to be physiological. Unbound plasma concentrations for oxycodone were extrapolated from the total plasma concentrations using the free fraction (59%) obtained from literature for healthy subjects (Dean, 2004; Kirvela et al., 1996).

#### 2.1.3. Morphine

Morphine human PK data in plasma and in $brain_{ECF}$ (study M1 and M2) were obtained from bilateral microdialysis measurements from both the injured and uninjured brain sides of TBI patients, thereby providing a comparison of physiological and pathophysiological conditions (Bouw et al., 2001; Ederoth et al., 2003). For both datasets, the unbound plasma concentrations were reported in these original publications.

#### 2.1.4. Phenytoin

Phenytoin human PK data in plasma and in $CSF_{SAS\_LUMBAR}$ (study P1) were obtained from epileptic patients, which were considered a pathophysiological CNS condition (Wilder et al., 1977). Unbound plasma concentrations for phenytoin were extrapolated from the total plasma concentrations using the free fraction (13%) obtained from literature for healthy subjects (Fraser et al., 1980), because the protein binding for healthy subject and for epileptic patients is similar (Peterson et al., 1982).

### 2.2. Human plasma PK models

For acetaminophen (study A3) and morphine (study M1 and M2), we used published human plasma PK models (Yamamoto et al., 2017c). For acetaminophen (study A1 and A2), oxycodone (study O1) and phenytoin (study P1), plasma PK models were systematically developed with a mixed effects modeling approach using available individual human plasma data (Table 1), since there is no plasma PK model from literature or the existing plasma PK model did not adequately describe the data (Yamamoto et al., 2017c). One-, two- and three-compartment models were evaluated for their utility to describe the data. Inter-individual variability was incorporated on each PK parameter, using an exponential model. Proportional and combined additive-proportional residual error models were tested. Model selection was guided by a likelihood ratio test with $p < 0.05$, the precision of the parameter estimates, assessment of the parameter correlation matrix, and graphical evaluation of the plots for observations *versus* predictions, weighted residuals *versus* time, and weighted residuals *versus* predictions (Nguyen et al., 2016).

### 2.3. Scaling of the rat CNS PBPK model to humans

The previously developed rat CNS PBPK model (Yamamoto et al., 2017b) (Fig. 1) consists of nine compartments, being plasma, brain microvessels, $brain_{ECF}$, $brain_{ICF}$, lysosomes, $CSF_{LV}$, CSF in the third and fourth ventricle ($CSF_{TFV}$), CSF in the cisterna magna ($CSF_{CM}$) and $CSF_{SAS\_LUMBAR}$. The model parameters are either system- or drug-specific.

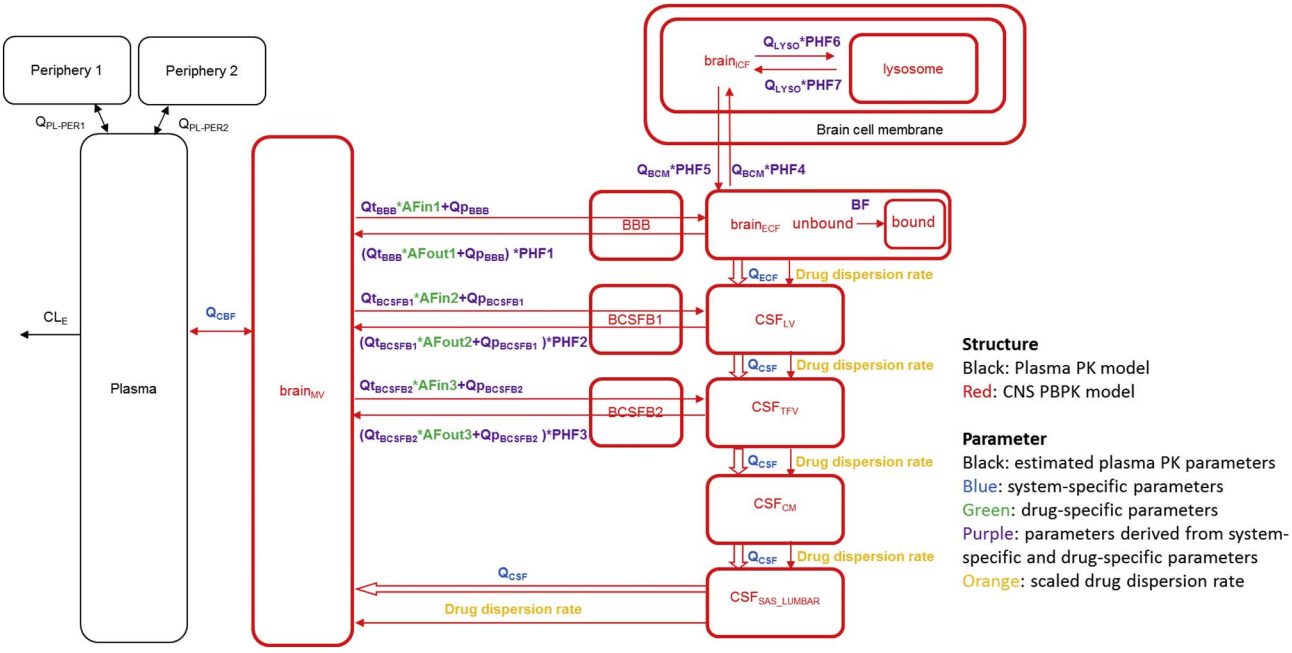


**Fig. 1.** The human PBPK model structure.
The model consists of a plasma PK model and a CNS PBPK model with estimated plasma PK parameters, and system-specific and drug-specific parameters (colors) for CNS. The plasma PK model was extended with peripheral compartments 1 and 2 in cases where these compartments were required to describe the plasma data adequately. $Brain_{MV}$: brain microvascular, BBB: blood-brain barrier, BCSFB: blood-CSF (*cerebrospinal fluid*) barrier, $brain_{ECF}$: brain extra cellular fluid, $brain_{ICF}$: brain intra cellular fluid, $CSF_{LV}$: CSF in the lateral ventricle, $CSF_{TFV}$: CSF in the third and fourth ventricle, $CSF_{CM}$: CSF in the cisterna magna, $CSF_{SAS\_LUMBAR}$: CSF in the subarachnoid space and lumbar region, $Q_{CBF}$: cerebral blood flow, $Qt_{BBB}$: transcellular diffusion clearance at the BBB, $Qp_{BBB}$: paracellular diffusion clearance at the BBB, $Qt_{BCSFB1}$: transcellular diffusion clearance at the BCSFB1, $Qp_{BCSFB1}$: paracellular diffusion clearance at the BCSFB1, $Qt_{BCSFB2}$: transcellular diffusion clearance at the BCSFB2, $Qp_{BCSFB2}$: paracellular diffusion clearance at the BCSFB2, $Q_{BCM}$: passive diffusion clearance at the brain cell membrane, $Q_{LYSO}$: passive diffusion clearance at the lysosomal membrane, $Q_{ECF}$: $brain_{ECF}$ flow, $Q_{CSF}$: CSF flow, AFin1–3: asymmetry factor into the CNS compartments 1–3, AFout1–3: asymmetry factor out of the CNS compartments 1–3, PHF1–7: pH-dependent factor 1–7, BF: binding factor. (For interpretation of the references to color in this figure legend, the reader is referred to the web version of this article.)

This rat CNS PBPK model was scaled to humans by 1) substitution of the rat system-specific parameters values by their corresponding human equivalents, 2) rat to human conversion of the contribution of active transport at the BBB and the BCSFB based on reported differences in the expression of active transporters, and 3) adding the rate of drug dispersion in the CNS.

### 2.3.1. System-specific parameters

Literature values were used for the physiological volumes for all CNS compartments, CBF, $brain_{ECF}$ bulk flow, CSF flow, surface area (SA) of the BBB ($SA_{BBB}$), SA of the BCSFB ($SA_{BCSFB}$), the ratio of $SA_{BBB}$ and $SA_{BCSFB}$ for transcellular and paracellular diffusion, the diameter of brain parenchyma cells, the diameter of lysosomes, the width of the BBB cells from brainMV to $brain_{ECF}$ and the effective pore size (Abbott et al., 2010; Adam and Greenberg, 1978; Begley et al., 2000; Cornford and Hyman, 2005; Dekaban and Sadowsky, 1978; Fagerholm, 2007; Ito et al., 2006; Kimelberg, 2004; Monteiro and Goraksha, 2017; Pardridge, 2011; Rengachary and Ellenbogen, 2005; Robertson, 1949; Sakka et al., 2011; Stange et al., 1997; Thorne et al., 2004; Wong et al., 2013). The $SA_{BCFSB}$ was divided into $SA_{BCSFB1}$ which is the SA around $CSF_{LV}$, and $SA_{BCSFB2}$ which is SA around $CSF_{TFV}$, like those in the rat CNS PBPK model (Yamamoto et al., 2017b). The total volume of lysosomes ($V_{LYSO}$) was calculated using the volume ratio of the lysosomes to the brain intracellular fluid of brain parenchyma cells (1:80) which was reported in rats (Loryan et al., 2014). In human, the volume of brain intracellular fluid ($Vbrain_{ICF}$) is 960 mL (Thorne et al., 2004), therefore $V_{LYSO}$ was calculated to be 12 mL. The SA of total brain parenchymal cell membrane and the SA of total lysosomes were calculated using the diameter of brain parenchyma cells and the volume of $brain_{ICF}$, and diameter of lysosomes and the total volume of lysosomes, respectively. The values of the system-specific parameters used in the model are summarized in Table 2.

### 2.3.2. Drug-specific parameters

The calculation of drug-specific parameters including the aqueous diffusivity coefficient and BBB transmembrane permeability of the compound was performed as described previously (Yamamoto et al., 2017b) and the details for the calculation are described in Supplementary material S1. In short, the aqueous diffusivity coefficient was calculated using the molecular weight of each compound (Avdeef et al., 2004), and transmembrane permeability was calculated using the log P of each compound (Grumetto et al., 2016). The influence of the net effect of active transporters on the drug exchange at the BBB and BCSFB was incorporated into the model using three asymmetry factors (AFin1–3 or AFout1–3, which can be calculated from Kp,uu values (unbound brain/CSF-to-plasma concentration ratio), such that they produced the same Kp,uu values within the model). If the net transport is influx of the drug, AFin1–3 were used, while AFout1–3 were fixed to 1. If the net transport is efflux of the drug, AFout1–3 were used, while AFin1–3 were fixed to 1 (Yamamoto et al., 2017b).

As no direct information is available on the values of AFs for human, we used two different approaches to obtain the values depending on the information available for the active transporters for each compound. We propose a workflow and decision tree to obtain human AF values for the individual compounds, based on availability of literature information (Fig. 2), as follows:

1) A literature search was performed for the main transporters involved in the BBB/BCSFB transport of the compounds in humans.
2) If relevant active transporters were reported, a literature search was performed on species differences in transporter protein expression/activity of the main active transporters.
3) If information on the inter-species differences was available, rat AF values were converted to human AF values using a conversion factor as calculated from the differences in transporter protein expression

**Table 1**
Summary of human plasma, brain and CSF data sources for the PBPK model evaluation.

| | | Acetaminophen | | | Oxycodone | Morphine | | Phenytoin |
|---|---|---|---|---|---|---|---|---|
| **Study design** | | *Study A1* | *Study A2* | *Study A3* | *Study O1* | *Study M1* | *Study M2* | *Study P1* |
| Condition of patients | | Healthy subjects | Patients with nerve-root compression | Patients with traumatic brain injury | Patients undergoing elective gynecological surgery | Patients with traumatic brain injury | Patients with traumatic brain injury | epileptic patients |
| Nr of subjects | | 1 (mean values) | 1 (mean values) | 7 | 12 | 2 | 1 | 6 |
| Dosage | | 1 g, 15 min infusion | 2 g (propacetamol), short infusion | 1 g, 30 min infusion | 0.1 mg/kg, 5 min infusion | 10 mg, 10 min infusion | 10 mg, 10 min infusion | 9.3-12.5 mg/kg, 35.0-92.8 mg/min |
| Nr of samples (sampling time, h) | plasma | 8 (0-6h) | 11 (0-12h) | 38 (0-6h) | 133 (0-24h) | 23 (0-3h) | 11 (0-3h) | 24 (0-1.25h) |
| | $brain_{ECF}$ [a] or CSF | 8 (0-6h) | 11 (0-13h) | 54 (0-5.5h) | 116 (0-24h) | 74 (0-3h) | 37 (0-3h) | 20 (0-1.25h) |
| **Data** | | | | | | | | |
| plasma | | X | X | X | X | X | X | X |
| $brain_{ECF}$ | | | | | | X [e], X [f] | X [e], X [f] | |
| $CSF_{EVD}$ [b] | | | | X | | | | |
| $CSF_{SAS\_LUMBAR}$ [c] | | X | X | | X | | | X |
| data references | | (Singla et al., 2012) | (Bannwarth et al., 1992) | (Yamamoto et al., 2017) | (Kokki et al., 2014) | (Ederoth et al., 2003) | (Bouw et al., 2001) | (Wilder et al., 1977) |
| fu,p [d] | | 85% | | | 59% | - | - | 13% |
| fu,p references | | (Gazzard et al., 1973) | | | (Dean, 2004)(Kirvela et al., 1996) | | | (Fraser et al., 1980) |

Blue: data was obtained under physiological CNS conditions, red: data was obtained under pathophysiological CNS conditions.
[a]Brain extracellular fluid compartment.
[b]Compartment of cerebrospinal fluid in EVD.
[c]Compartment of cerebrospinal fluid in subarachnoid space and lumbar region.
[d]Free fraction in plasma.
[e]Better side of brain tissue.
[f]Injured side of brain tissue.

and/or activity of the main active transporters between rats and humans (Method 1).

4) If information of the inter-species differences was not available for the compound, we searched information available from other compounds whose transfer are predominantly mediated by the same transporters, and then step 2 was repeated (Method 2).
5) If an active transporter was not reported, we searched for *in vitro* data able to derive the net contribution of active transport component on the overall permeability. If no indications of active transport could be found, the human AF values were fixed to 1 (Method 3). The details of the calculation methods to obtain human AF values from the *in vitro* data are described in Supplementary material S3.

Below we describe in detail the rationale for selection of AF values for each compound.

*2.3.2.1. Acetaminophen.* Acetaminophen is reported to be transported across the human BBB by passive diffusion only, (Mabondzo et al., 2010), therefore we fixed the AF values for acetaminophen to 1 (Method 3).

*2.3.2.2. Oxycodone.* An active influx transporter for oxycodone at the BBB has been reported; pyrilamine-sensitive proton-coupled organic cation (H + /OC) antiporter (Okura et al., 2008; Shimomura et al., 2013). Even though information on species difference in its protein expression level and its activity is not directly available for oxycodone, the transporter activity can be deduced from the *in vitro* observations on pyrilamine transfer, of which the exchange at the BBB is predominantly mediated by this transporter (Okura et al., 2008; Shimomura et al., 2013). Therefore, Method 2 was applied for oxycodone. According to the *in vitro* studies on pyrilamine in the human BBB model (hCMEC/D3 cells), the Km and Vmax values of active uptake are comparable to those in the rat BBB model (TR-BBB13 cells) (Shimomura et al., 2013). Moreover, the weaker active uptake of oxycodone comparing to that of pyrilamine in the human BBB model (Shimomura et al., 2013) is in line with the observations in the rat BBB model (Okura et al., 2008). It thus appears reasonable to assume that the BBB influx mediated by this transporter is comparable between rat and human, and therefore the human AFs were considered to be similar to rat AFs. The human AF at the BBB, AFin1, was 2.3, which was calculated using a $Kpuu,brain_{ECF}$ (unbound $brain_{ECF}$-to-plasma concentration ratio) value of 1.7 (Kitamura et al., 2016). The human AFs at the BCSFB, AFout2 and AFout3, were assumed to be 1.9 and 2.3, respectively, which were calculated from a Kpuu,CSF (unbound CSF-to-plasma concentration ratio) value of 1 (Kokki et al., 2014).

*2.3.2.3. Morphine.* Permeability glycoprotein (P-gp) and multidrug resistance-associated proteins (MRPs) are reported to be the active efflux transporters for morphine at the rat BBB (Letrent et al., 1999; Tunblad et al., 2003). Furthermore, an involvement of active influx transporters has also been suggested in rat BBB (Groenendaal et al., 2007). Even though morphine is reported to be a substrate of P-gp (Wandel et al., 2002) for humans, other efflux and influx transporters have not been clearly identified. The P-gp protein concentration in rat brain endothelial cells is about 19 fmol/mg protein, which is about three-fold higher than that in humans (6 fmol/mg protein) (Aday et al.,

**Table 2**
System-specific parameters of the human PBPK model in healthy condition.

| Description | | Parameter | Human value | Reference |
|---|---|---|---|---|
| Volumes | Brain | $V_{tot}$ | 1400 mL | (Dekaban and Sadowsky, 1978) |
| | $Brain_{ECF}$ | $Vbrain_{ECF}$ | 240–280 mL (260 was used in the model) | (Begley et al., 2000; Thorne et al., 2004) |
| | $Brain_{ICF}$ | $Vbrain_{ICF}$ | 960 mL | (Thorne et al., 2004) |
| | Total lysosome | $V_{LYSO}$ | 12 mL | calculated[d] |
| | $CSF_{LV}$ | $VCSF_{LV}$ | 20–25 mL (22.5 was used in the model) | (Pardridge, 2011; Sakka et al., 2011) |
| | $CSF_{TFV}$ | $VCSF_{TFV}$ | 20–25 mL (22.5 was used in the model) | (Pardridge, 2011; Sakka et al., 2011) |
| | $CSF_{CM}$ | $VCSF_{CM}$ | 7.5 mL | (Adam and Greenberg, 1978; Robertson, 1949) |
| | $CSF_{SAS\_LUMBAR}$ | $VCSF_{SAS\_LUMBAR}$ | 90–125 mL (90 was used in the model) | (Pardridge, 2011; Sakka et al., 2011) |
| | Brain microvascular | $V_{MV}$ | 150 mL | (Rengachary and Ellenbogen, 2005) |
| Flows | Cerebral blood flow | $Q_{CBF}$ | 610–860 mL/min (735 was used in the model) | (Fagerholm, 2007; Ito et al., 2006; Stange et al., 1997) |
| | $Brain_{ECF}$ bulk flow | $Q_{ECF}$ | 0.15–0.2 mL/min (0.175 was used in the model) | (Kimelberg, 2004) |
| | CSF flow | $Q_{CSF}$ | 0.3–0.4 mL/min (0.35 was used in the model) | (Kimelberg, 2004) |
| Surface areas | BBB | $SA_{BBB}$ | 12–18 $m^2$[a] (12 was used in the model) | (Abbott et al., 2010; Wong et al., 2013) |
| | BCSFB | $SA_{BCSFB}$ | 6–9 $m^2$[b,c] (7.5 was used in the model) | calculated (assumed 50% of $BBB_{SA}$) |
| | Total BCM | $SA_{BCM}$ | 228 $m^2$ | calculated[e] |
| | Total lysosomal membrane | $SA_{LYSO}$ | 180 $m^2$ | calculated[f] |
| Width | BBB | $Width_{BBB}$ | 0.3–0.5 μm (0.5 was used in the model) | (Cornford and Hyman, 2005) |
| Effective pore size | BBB | | 0.0007–0.0009 μm (0.0007 was used in the model) | (Monteiro and Goraksha, 2017) |

CSF, cerebrospinal fluid; BBB, blood-brain barrier; BCSFB, blood-cerebrospinal barrier; BCM, brain cell membrane.
[a] 99.8% of $SA_{BBB}$ was used for transcellular diffusion, and 0.004% of $SA_{BBB}$ was used for paracellular diffusion.
[b] 99.8% of $SA_{BCSFB}$ was used for transcellular diffusion and 0.016% of $SA_{BCSFB}$ was used for paracellular diffusion.
[c] $SA_{BCSFB1}$ and $SA_{BCSFB2}$ was both assumed to be 3.75 $cm^2$.
[d] Based on the volume ratio of lysosomes to $brain_{ICF}$ (1:80).
[e] Based on the number of brain parenchyma cells which was calculated using the total $brain_{ICF}$ volume and diameter of each brain parenchyma cell (15 μm) (Trapa et al., 2016).
[f] Based on the lysosome number per cell which was calculated using the total lysosomal volume and diameter of each lysosome (0.5–1.0 μm) (Hardin et al., 2011).

2016). Regarding the P-gp activity for morphine, no inter-species difference has been observed (Feng et al., 2008). Therefore, the rat-to-human conversion factor of AFs was set to 3 for morphine. The rat AFout1, AFout2 and AFout3 are 20, 38 and 49, respectively (Yamamoto et al., 2017b), and therefore in this study human AFout1, AFout2 and AFout3 were assumed to be 6.6, 13 and 16, respectively (Method 1).

*2.3.2.4. Phenytoin.* P-gp and MRPs are suggested to be the active efflux transporters for phenytoin at the rat BBB (Potschka and Löscher, 2001a; Potschka and Löscher, 2001b). However, many *in vitro* studies, including the studies using human hCMEC/D3 cells and other cells expressing human P-gp and human MRPs, have shown that phenytoin is neither a substrate for human P-gp nor human MRP2 (Baltes et al., 2007; Dickens et al., 2013; Luna-Tortós et al., 2010; Zhang et al., 2010).

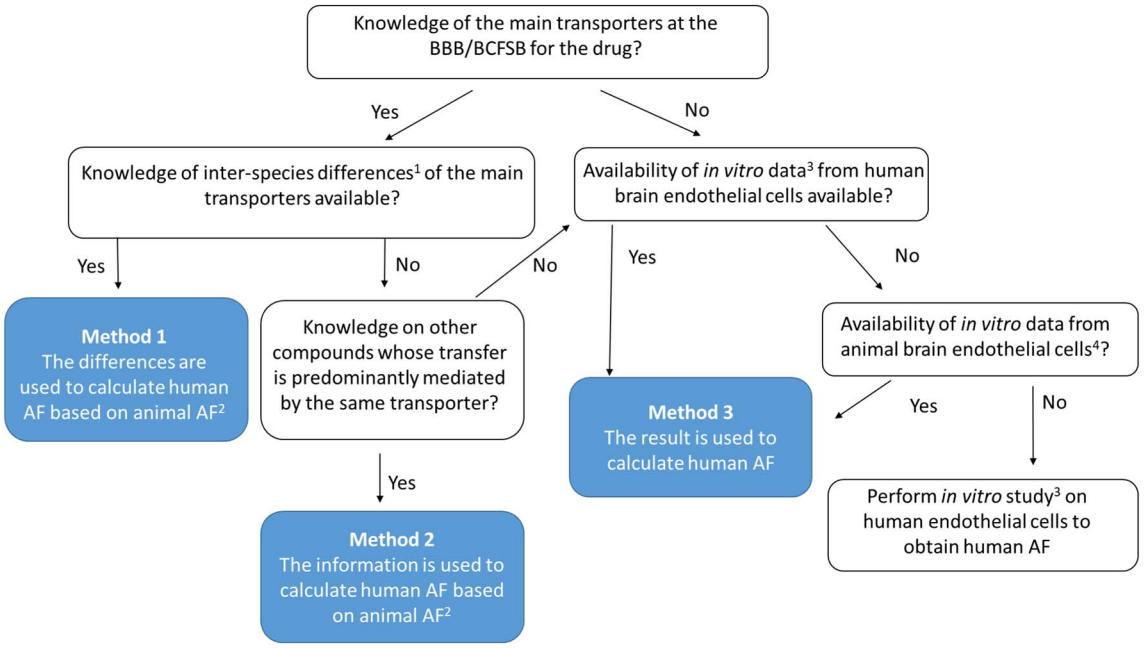


1. Inter-species differences of the expression level and activity/function of the main transporters, are needed.
2. The methods to calculate the rat AF were reported (Yamamoto et al., 2017b). In short, rat AF was calculated using the Kp,uu values which were obtained from *in vivo* studies or *in silico* predictions.
3. *In vitro* data which is able to derive active transport component of the overall permeability are needed. The details are provided in supplementary material S3.
4. The assumption is made that the overall active transport characteristics of animal and human BBB are similar.

**Fig. 2.** Decision tree to obtain human AFs.

Even though the reasons for these differences between the *in vivo* rat studies and the *in vitro* experiments using human P-gp and MRPs are not clear, inter-species differences in the activity by P-gp for phenytoin (Baltes et al., 2007) and MRP2 have been reported (Li et al., 2008). Therefore, Method 3 was applied to predict AFs for phenytoin. In this study, we assumed that the human AFs for phenytoin are equal to 1.

#### 2.3.3. Use of system-specific and drug-specific parameters in the model

Drug transport at the BBB and BCSFB, brain cellular distribution, acidic subcellular distribution and drug binding were derived by using drug-specific parameter values and system-specific parameters. The equations to obtain above parameters have been described previously (Yamamoto et al., 2017b), therefore the details are provided in Supplementary material S2. In short, drug transport at the BBB and BCSFB were calculated using passive diffusion clearance at the BBB and BCSFB of each compound, $SA_{BBB}$ and $SA_{BCSF}$ and the influence of the net effect of active transporters at the BBB and BCSF. Brain cellular distribution including acidic subcellular distribution was taken into account in the model using passive diffusion clearance at brain cell membrane (BCM) and lysosomal membrane of each compound, SA of BCM and lysosomal membrane, pKa of each compound and pH in each CNS compartment. Finally, drug binding was calculated using log P of each compound and composition of human brain tissue.

#### 2.3.4. Scaling of the dispersion rate

Previously the values of the system-specific drug dispersion rate within the brain and CSF have been estimated based on rat microdialysis data of nine compounds (Yamamoto et al., 2017c). This dispersion rate is defined as a combination of CSF flow, $brain_{ECF}$ bulk flow and turbulence flow of the drug molecules. For the scaling of the drug dispersion rate to humans we used the following allometric scaling equation.

$$P_{human} = P_{rat} \times \left(\frac{BW_{human}}{BW_{rat}}\right)^{0.75} \quad (1)$$

where $P_{human}$ is the scaled human parameter, $P_{rat}$ is the estimated rat parameter from the model, $BW_{human}$ is the average human body weight (75 kg), and $BW_{rat}$ is the average rat body weight (250 g).

### 2.4. Evaluation of the human CNS PBPK model

The predictions of the scaled human CNS PBPK model were evaluated by comparing of model predictions to observed human PK data in $brain_{ECF}$, $CSF_{SAS\_LUMBAR}$ and/or $CSF_{EVD}$ (Table 1). The accuracy of the prediction was evaluated with symmetric mean absolute percentage error (SMAPE) (Eq. (2)) using population prediction (PRED). We also performed 200 simulations for each compound, then calculated 2.5% tile, median and 97.5% tile of the simulated concentrations and plotted these together with the observations.

$$SMAPE = \frac{1}{N}\sum_{k=1}^{N}\left|\frac{Y_{OBS,ij} - Y_{PRED,ij}}{(Y_{OBS,ij} + Y_{PRED,ij})/2}\right| \times 100 \quad (2)$$

where $Y_{OBS,ij}$ is the *j*th observation of the *i*th subject, $Y_{PRED,ij}$ is the *j*th mean prediction of the *i*th subject, and N is the number of observations.

### 2.5. Simulated impact of different pathophysiological conditions on CNS PK

Under pathophysiological CNS conditions, several CNS system-specific parameter values, such as CBF, BBB characteristics, BCSFB characteristics, $brain_{ECF}$ bulk flow, CSF flow and active transporters, have been reported to be changed (Supplemental Table S1). The following data were available from literature: acetaminophen concentrations in $CSF_{EVD}$ and morphine concentrations in $brain_{ECF}$ which were obtained from TBI patients, and phenytoin data in $CSF_{SAS\_LUMBAR}$ which were obtained from epileptic patients (Table 1).

In TBI patients, a decrease in CBF, an increase in paracellular permeability due to the disruption of the tight junction complexes, and changes in activity/expression of active transporters (such as a decreased expression of P-gp) have been reported (Chodobski et al., 2011; Greve and Zink, 2009; Pop et al., 2013). For epileptic conditions, studies have indicated regional decreases in CBF, increased paracellular permeability due to the opening of the tight junction proteins, and an increase in some active efflux transporters such as P-gp and MRPs (Appel et al., 2012; Bednarczyk and Lukasiuk, 2011; Lazarowski et al., 2007; Löscher and Potschka, 2002).

To investigate the impact of such pathological changes on PK profiles of each compound, we simulated the PK upon such changes. In the simulations, the system-specific parameter values were varied within a range of 20–500% of their original values (*i.e.* 5 times lower or higher).

If the changes in the values of the system-specific parameters had a relevant impact on PK profiles, the model predictions were performed again by adapting values of system-specific parameters identified in the literature, and subsequently compared to the observed PK data.

## 3. Results

### 3.1. Plasma PK parameter values

The plasma PK parameters used in the analysis for acetaminophen, morphine, oxycodone, and phenytoin are summarized in Supplemental Table S2 (relative standard error < 66%). For acetaminophen (study A3) and morphine (study M1 and M2), the plasma PK parameter values were obtained from literature (Yamamoto et al., 2017c). For acetaminophen (study A1 and study A2), oxycodone (study O1) and phenytoin (study O1), the descriptive plasma PK model was developed using available plasma data. One-compartment model, two-compartment model and two-compartment model could describe very well the available PK data for acetaminophen, oxycodone and phenytoin respectively (Figs. 3 and 5).

### 3.2. Prediction of CNS PK in physiological CNS conditions

All CNS PBPK model parameters were either derived from *in silico* predictions, literature data or based on *in vitro* information. System-specific and drug-specific parameters in physiological CNS conditions are summarized in Tables 2 and 3, respectively. The parameters derived from human system-specific and drug-specific parameters are summarized in Table 4. The drug dispersion rate for human was calculated to be 1.6 mL/min based on allometric scaling. The model could adequately predict the PK profiles in $brain_{ECF}$ for morphine and the PK profiles in $CSF_{SAS\_LUMBAR}$ for acetaminophen and oxycodone under physiological CNS conditions (Fig. 3), with an SMAPE of $brain_{ECF}$ and $CSF_{SAS\_LUMBAR}$ of 49% and 54%, respectively.

### 3.3. Prediction of CNS PK in TBI and epileptic conditions

To explore the impact of each system-specific parameters, which were altered in pathological CNS conditions of TBI and epilepsy on the PK profiles for acetaminophen, morphine and phenytoin, simulations were performed by changing the values of the CBF, and paracellular diffusion. The influence of the active efflux transporters was also simulated for morphine. The impact on model predictions after changing the values of CBF, paracellular diffusion and the influence of the active efflux transporters within a range of 20–500% of their original values are shown in Fig. 4. It can be seen that the impact of pathological changes on PK profiles is drug-dependent and CNS compartment-dependent. For acetaminophen, the PK profiles in $CSF_{LV}$ were not sensitive to the changes in CBF nor to the changes in paracellular diffusion across the BBB/BCSFB. In contrast, for morphine $brain_{ECF}$ concentrations increased with an increase in paracellular diffusion, and decreased with an increase in active efflux transport. For phenytoin, no change

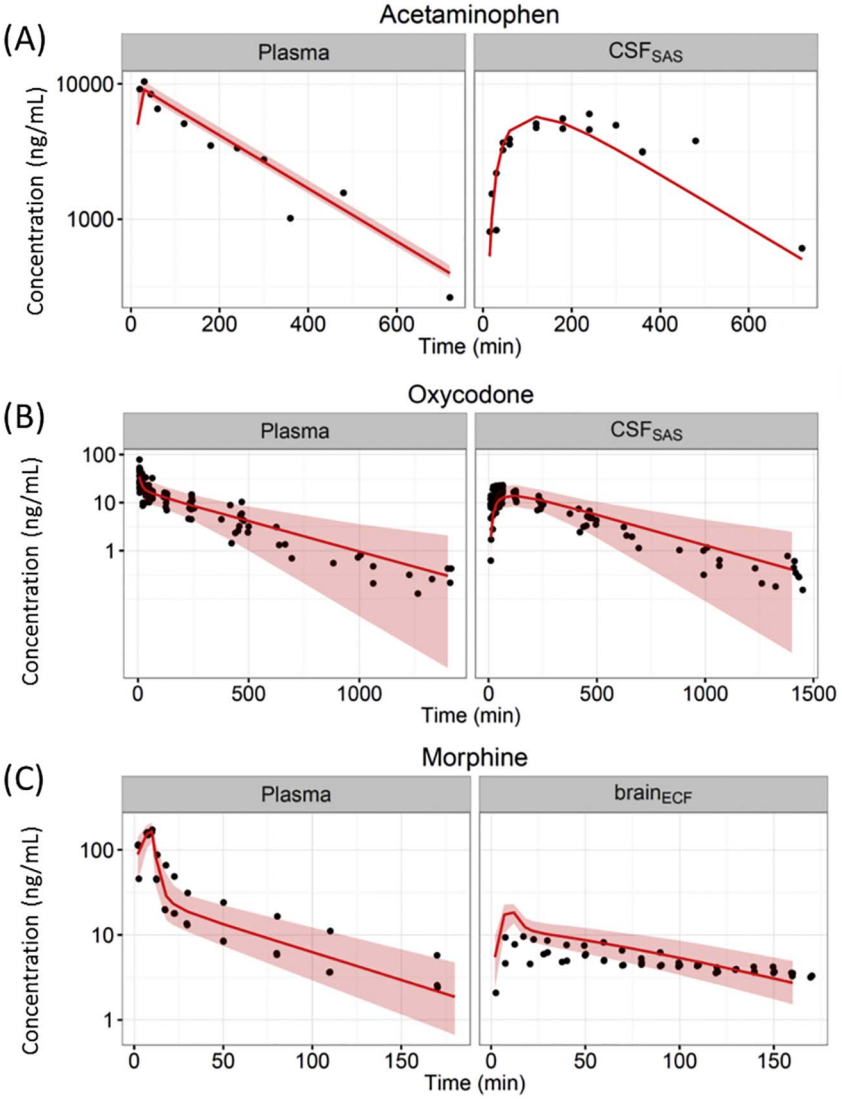


**Fig. 3.** Predicted (red lines: median, shaded area is 95 % prediction interval) and observed (circles) concentration-time profiles in CNS compartments under physiological conditions. (A) Plasma and CSF in the lumbar region ($CSF_{SAS\_LUMBAR}$) data for acetaminophen which were obtained from both healthy subjects and patients with nerve-root compression, (B) plasma and $CSF_{SAS\_LUMBAR}$ data for oxycodone which were obtained from patients undergoing elective gynecological surgery and (C) plasma and $brain_{ECF}$ data for morphine which were obtained from the uninjured side of the brain in traumatic brain injury (TBI) patients. The x-axis represents the time in minutes and the y-axis represents the concentration in ng/mL. (For interpretation of the references to color in this figure legend, the reader is referred to the web version of this article.)

was observed in PK profiles in $CSF_{SAS\_LUMBAR}$ with the changes in CBF and paracellular diffusion.

Since TBI and epilepsy conditions did not influence acetaminophen PK profiles in $CSF_{LV}$ and phenytoin PK profiles in $CSF_{SAS\_LUMBAR}$ to a significant extent, the model prediction for these PK data was performed using the physiological values of the system-specific parameters (Fig. 5). The model predictions captured the acetaminophen PK data in $CSF_{EVD}$ and the phenytoin PK data in $CSF_{SAS\_LUMBAR}$ well even if the concentrations are slightly over-predicted around the early sampling time for the acetaminophen PK data in $CSF_{EVD}$.

On the other hand, we found that the values of paracellular diffusion and the influence of the active efflux transporters needed to be adjusted to capture the morphine concentrations in $brain_{ECF}$ in TBI patients (Fig. 4). Morphine PK data in $brain_{ECF}$ in TBI patients were captured well when paracellular diffusion was upregulated and active efflux transport was downregulated (Fig. 6).

## 4. Discussion

We developed a human CNS PBPK model to predict unbound drug PK of four model compounds in multiple CNS compartments. Under physiological CNS conditions, good predictions of observed human data were achieved within a 1.6-fold error. Furthermore, the model showed its ability to be used for building a better understanding of the key system properties that may explain the changes on drug concentration-time profiles under pathophysiological CNS conditions.

The human CNS PBPK model can be applied to any (existing or new) compounds once the physicochemical properties and information on the involvement of active transporters at the BBB and the BCSFB are available. Such information can be obtained from *in silico* predictions and/or *in vitro* studies.

The model uses plasma PK data as input to build a plasma PK model. In our study we either used previously published plasma PK models or we developed the plasma PK model separately on the basis of existing plasma PK data, which described the available human plasma PK data to the best possible extent. It should be noted that even in the absence of a plasma PK model or plasma PK data, the CNS PBPK model can be used in conjunction with plasma PK simulations by using the existing whole-body PBPK platforms. Thus, the human CNS PBPK model does not require any *in vivo* data to predict unbound drug PK at target-site in the human CNS.

Gathering as much information as possible about unbound drug PK in the CNS is important to improve CNS drug development and CNS drug treatment, because it is the driver for drug-target binding kinetics and therewith for the drug effect profile. In contrast to the *ex vivo* techniques, such as brain homogenate and brain slicing techniques, as well as *in silico* approaches like quantitative structure-activity relationship models (Chen et al., 2011; Loryan et al., 2015) that can

**Table 3**
Drug-specific parameters of the PBPK model.

| | | | Acetaminophen | Oxycodone | Morphine | Phenytoin |
|---|---|---|---|---|---|---|
| Drug specific parameters | | | | | | |
| Transmembrane permeability | | cm/min | $1.1 * 10^{-4}$ | $3.5 * 10^{-4}$ | $2.5 * 10^{-4}$ | 0.0077 |
| Aqueous diffusivity coefficient (paracellular diffusion) | | $cm^2$/min | $4.6 * 10^{-4}$ | $3.3 * 10^{-4}$ | $3.4 * 10^{-4}$ | $3.6 * 10^{-4}$ |
| AF | AFin1 | | 1 | 2.3 | 1 | 1 |
| | AFin2 | | 1 | 1 | 1 | 1 |
| | AFin3 | | 1 | 1 | 1 | 1 |
| | AFout1 | | 1 | 1 | 6.6 | 1 |
| | AFout2 | | 1 | 1.9 | 13 | 1 |
| | AFout3 | | 1 | 2.3 | 16 | 1 |
| Free fraction | | | | | | |
| fu,p | | | 0.85 | 0.59 | 0.11 | 0.13 |
| fu,b | | | – | 0.39 (Ball et al., 2012) | 0.45 (Ball et al., 2012) | – |
| Physicochemical properties | | | | | | |
| Molecular weight | | | 151 | 315 | 285 | 252 |
| log P | | | 0.5 | 1.0 | 0.9 | 2.5 |
| pKa (acid) | | | 9.5 | 13.6 | 10.3 | 9.5 |
| pKa (base) | | | − 4.4 | 8.2 | 9.1 | − 9.0 |
| Charge class | | | Neutral | Base | Base | Neutral |

AF, asymmetry factor.
AFin1–3 and AFout1–3 were converted from the rat AFs or obtained from *in vitro* study.

**Table 4**
Parameters derived using system-specific and drug-specific parameters in the PBPK model.

| Parameter | Unit | Acetaminophen | Oxycodone | Morphine | Phenytoin |
|---|---|---|---|---|---|
| $Q_{BBB\_in}$ | mL/min | 72 | 120 | 64 | 510 |
| $Q_{BBB\_out}$ | mL/min | 72 | 68 | 130 | 510 |
| $Qt_{BBB}$ | mL/min | 6.5 | 21 | 15 | 460 |
| $Qp_{BBB}$ | mL/min | 66 | 47 | 50 | 52 |
| PHF1 | | 1.0 | 0.82 | 0.80 | 1.0 |
| $Q_{BCSFB1\_in}$ | mL/min | 57 | 47 | 46 | 190 |
| $Q_{BCSFB1\_out}$ | mL/min | 57 | 46 | 98 | 190 |
| $Qt_{BCSFB1}$ | mL/min | 2.0 | 6.6 | 4.7 | 140 |
| $Qp_{BCSFB1}$ | mL/min | 55 | 39 | 41 | 43 |
| PHF2 | | 1.0 | 0.82 | 0.80 | 1.0 |
| $Q_{BCSFB2\_in}$ | mL/min | 57 | 47 | 46 | 190 |
| $Q_{BCSFB2\_out}$ | mL/min | 57 | 46 | 98 | 190 |
| $Qt_{BCSFB2}$ | mL/min | 2.0 | 6.6 | 4.7 | 140 |
| $Qp_{BCSFB2}$ | mL/min | 55 | 39 | 41 | 43 |
| PHF3 | | 1.0 | 0.82 | 0.80 | 1.0 |
| $Q_{BCM\_in}$ | mL/min | 250 | 650 | 461 | 18,000 |
| $Q_{BCM\_out}$ | mL/min | 250 | 360 | 230 | 18,000 |
| PHF4 | | 1.0 | 0.82 | 0.80 | 1.0 |
| PHF5 | | 1.0 | 0.43 | 0.40 | 1.0 |
| $Q_{LYSO\_in}$ | mL/min | 120 | 170 | 120 | 8800 |
| $Q_{LYSO\_out}$ | mL/min | 130 | 1.8 | 1.2 | 8900 |
| PHF6 | | 1.0 | 0.43 | 0.40 | 1.0 |
| PHF7 | | 1.0 | 0.0046 | 0.0041 | 1.0 |
| BF | | – | 0.01 | 1 | – |

$Q_{BBB\_in} = Qp_{BBB} + Qt_{BBB} * AFin1$, $Q_{BBB\_out} = (Qp_{BBB} + Qt_{BBB} * AFout1) * PHF1$, $Qp_{BBB}$ = (Aqueous diffusivity coefficient / $Width_{BBB}$) * $SA_{BBBp}$, $Qt_{BBB} = 1/2 *$ Transmembrane permeability * $SA_{BBBt}$.
$Q_{BCSFB1\_in} = Qp_{BCSFB1} + Qt_{BCSFB1} * AFin2$, $Q_{BCSFB1\_out} = (Qp_{BCSFB1} + Qt_{BCSFB1} * AFout2) * PHF2$, $Qp_{BCSFB1}$ = (Aqueous diffusivity coefficient / $Width_{BCSFB1}$) * $SA_{BCSFB1p}$, $Qt_{BCSFB1} = 1/2 *$ Transmembrane permeability * $SA_{BCSFB1t}$.
$Q_{BCSFB2\_in} = Qp_{BCSFB2} + Qt_{BCSFB2} * AFin3$, $Q_{BCSFB2\_out} = (Qp_{BCSFB2} + Qt_{BCSFB2} * AFout3) * PHF3$, $Qp_{BCSFB2}$ = (Aqueous diffusivity coefficient / $Width_{BCSFB2}$) * $SA_{BCSFB2p}$, $Qt_{BCSFB2} = 1/2 *$ Transmembrane permeability * $SA_{BCSFB2t}$.
$Q_{BCM\_in}$ = Transmembrane permeability * $SA_{BCM}$ * PHF4, $Q_{BCM\_out}$ = Transmembrane permeability * $SA_{BCM}$ * PHF5.
$Q_{LYSO\_in}$ = Transmembrane permeability * $SA_{LYSO}$ * PHF6, $Q_{LYSO\_in}$ = Transmembrane permeability * $SA_{LYSO}$ * PHF7.
PHF1, PHF2, PHF3, PHF4, PHF5, PHF6, and PHF7 were calculated from the pKa of each compound and pH of the respective compartment.
BF was calculated from the Kp of each compound.

provide information on unbound concentrations in the brain at steady state conditions, the CNS PBPK model predicts the unbound drug concentration time course. This is an important improvement since even during chronic dosing, variations in drug concentrations will still be present and may influence the target occupancy-time profile (de Witte et al., 2016).

The human CNS PBPK model allows prediction of the unbound drug PK in multiple physiologically relevant CNS compartments. This is crucial as the PK profiles in different CNS compartments are known to be different, even for drugs that are not subjected to active transport (Westerhout et al., 2012). Moreover, the model could be used to investigate the impact on PK profiles in the different CNS compartments as a result of pathological processes, which have shown to be drug-dependent as well as CNS compartment-dependent (Figs. 5 and 6). To our best knowledge, such integration of multiple aspects has not been reported earlier, and it will substantially contribute to an increased insight into CNS PK changes in pathological conditions in relation to the CNS effects.

A key feature of drug transport across the BBB and BCSFB is the contribution of active transporters. In PBPK modeling, expression levels and activity of each active transporter should ideally be separately incorporated. The major transporters such as P-gp and MRP are investigated well with regard to their inter-species differences of expression levels and transporters activity; however, such information is currently lacking for the other transporters (Aday et al., 2016; Ohtsuki et al., 2013).

Therefore, in our human CNS PBPK model, instead of using information on individual transporters, we used the "net contribution of the active transport" approach. This is a useful approach in situations where active transporters, which have not yet been widely investigated, are involved in the process of drug exchange at the BBB/BCSFB. In this study, we investigated a method to convert the "net contribution of the active transport (AFs)" at the BBB and BCSFB from rat to human, or obtain it from *in vitro* studies. We propose a workflow and decision tree to derive human "net contribution of the active transport (AFs)" (Fig. 2).

In the rat PBPK model, we derived the "net contribution of the active transport (AFs)" from Kp,uu values (Yamamoto et al., 2017b). The translational method of AFs values from rat to human depends on the available information about the transporters involved in the processes. If the existing literature information is not sufficient to support the

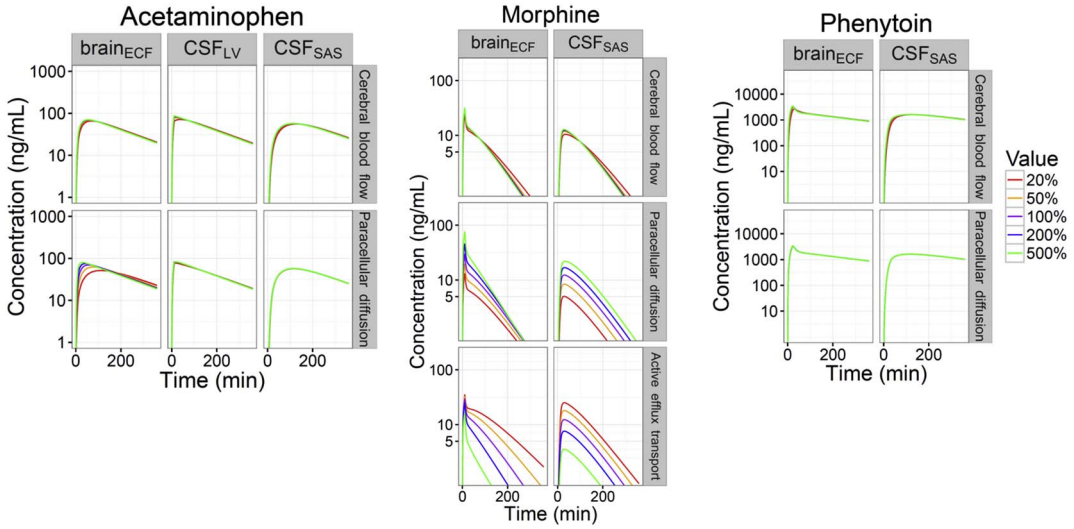


**Fig. 4.** Simulation of the concentration-time profiles for acetaminophen, morphine and phenytoin using the human CNS PBPK model. The values of CBF, paracellular diffusion and an influence of active transports (if applicable) were varied within the range of 20–500% of their original values (colors). The plots were stratified by the CNS compartments (panels). The x-axis represents the time in minutes and the y-axis represents the concentration in ng/mL. (For interpretation of the references to color in this figure legend, the reader is referred to the web version of this article.)

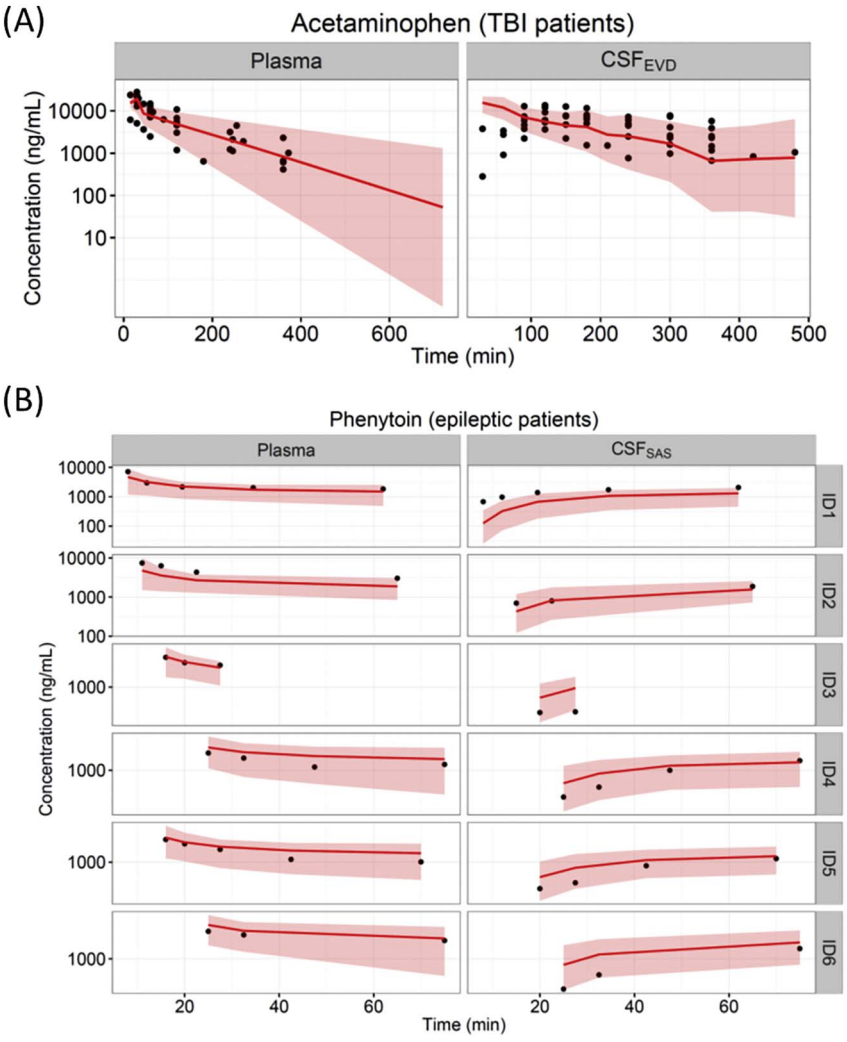


**Fig. 5.** Model prediction (red lines: median, shaded area is 95% prediction interval) versus concentration-time profiles (circles) for each pathophysiological condition. (A) Acetaminophen data was obtained from plasma and CSF in the lateral ventricle collected by extra-ventricular drainage ($CSF_{EVD}$) from traumatic brain injury (TBI) patients, (B) phenytoin data was obtained from plasma and CSF in the lumbar region ($CSF_{SAS\_LUMBAR}$) from epileptic patients. The x-axis represents the time in minutes and the y-axis represents the concentration in ng/mL. (For interpretation of the references to color in this figure legend, the reader is referred to the web version of this article.)

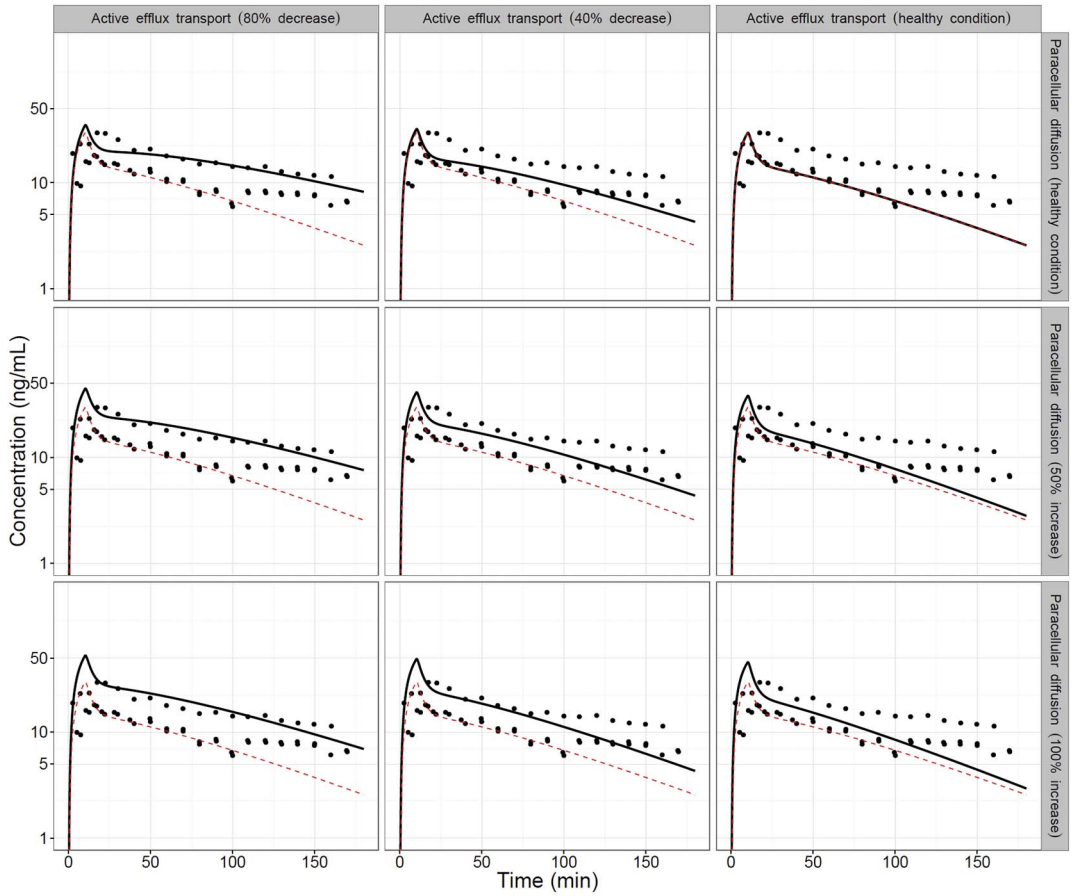


**Fig. 6.** Model prediction (black lines) versus concentration-time profiles (circles) for morphine in $brain_{ECF}$ in TBI patients. The plots were stratified by the change in the values of the system-specific parameters. The red dotted lines were the model predicted concentration-time profile for morphine in $brain_{ECF}$ in healthy subjects. The x-axis represents the time in minutes and the y-axis represents the concentration in ng/mL.

conversion of the rat AFs to human AFs, we proposed alternative methods to obtain human AFs directly from *in vitro* study using preferably human brain endothelial cells, such as hCMEC/D3 cells. Thus, either way, theoretically we do not need any *in vivo* data to obtain human AFs.

We have shown the potential of the model to be adapted according to literature information of pathophysiological changes and to explore the impact of the pathophysiological changes on PK profiles in each CNS compartment. For PK data for acetaminophen in $CSF_{EVD}$ under TBI condition and PK data for phenytoin in $CSF_{SAS\_LUMBAR}$ under epileptic conditions, the impact of the conditions did not lead to significant alterations of CNS PK, hence no change to the model was needed to obtain reasonable predictions. For morphine, the simulations showed that the model could describe the drug concentration in $brain_{ECF}$ in TBI patients if the paracellular diffusion at the BBB and BCSFB was increased by > 50% and AFs at the BBB and BCSFB were decreased by > 40%. Our findings align with the reported 40% decrease in expression of P-gp in TBI patients (Pop et al., 2013). This demonstrates how the model could provide quantitative mechanistic insights of clinically observed alterations in CNS PK which are supported by additional external evidence. In the future, additional human data, for example from the accessible CSF lumbar region, can provide further information to validate the model in other pathophysiological conditions, and can better inform the human CNS PBPK model about what system-specific parameter values has actually changed or how much the system-specific parameter values need to be adjusted.

Due to the lack of information for the drug dispersion rate in the CSF, we used allometric scaling of the drug dispersion rate in rats using body weight to obtain the drug dispersion rate for humans. Since the drug dispersion rate may be different depending on the physiological components such as the length of spine and size of the tube of spine, an allometric scaling can be considered as an appropriate approach to scale the value among species. In this study, the average drug dispersion rate value in rat for the nine compounds was used for the scaling (Yamamoto et al., 2017c). At least for acetaminophen, oxycodone, morphine and phenytoin, the average drug dispersion rate was sufficient to capture the PK profiles of the compounds in the CNS. However, the drug dispersion rate may depend on not only the physiological components (which have already been taken into account by the allometric scaling), but also on the physicochemical properties such as molecular weight and lipophilicity. Therefore, further investigations are needed to optimize the drug dispersion rate for each compound in human.

The CNS PBPK model was evaluated using the four compounds in this analysis. Due to ethical and practical constraints, it was difficult to obtain PK data in the $brain_{ECF}$ and CSF from many compounds. Even though the four compounds have distinctive physicochemical properties, further analysis using a larger dataset is expected to consolidate the CNS PBPK model predictive performance. Furthermore, differences in drug PK profiles between brain regions (such as striatum, cerebellum and hippocampus, *etc.*) have recently been reported due to the differences in the level of transporter-mediated transport and receptor density (de Witte et al., 2016; Loryan et al., 2016). Inclusion of regional brain physiological parameter values is one of the next steps in the CNS PBPK model development.

## 5. Conclusions

A human CNS PBPK model was developed to predict the concentration-time profiles of four model compounds in human CNS compartments. All model parameters were either derived from *in silico* predictions, literature data or based on *in vitro* information. Therefore, the model can provide the concentration-time profiles in multiple physiologically relevant compartments in human CNS without the need of *in vivo* PK data. We demonstrated that the model could predict the $brain_{ECF}$ and $CSF_{SAS\_LUMBAR}$ concentrations-time profiles under physiological CNS conditions. We also showed how the model can provide quantitative understanding of the impact of pathophysiological conditions on PK profiles in each CNS location. This human CNS PBPK model provides the basis to link CNS PK with drug-target binding kinetics and the biological effect(s) of the drug. As such, the developed model will have a substantial role in the selection of CNS drug candidates, in the prediction of target-site concentrations in humans, and to support the assessment of drug efficacy and safety in the early stage of the drug development.

## Conflict of interest/disclosure

The authors have no conflicts of interest that are directly relevant to the contents of this research article.

## Acknowledgments

This research article was prepared within the framework of project no. D2-501 of the former Dutch Top Institute Pharma, currently Lygature (Leiden, the Netherlands; www.lygature.org).

## Appendix A. Supplementary data

Supplementary data to this article can be found online at https://doi.org/10.1016/j.ejps.2017.11.011.

## References

Abbott, N.J., Patabendige, A.A.K., Dolman, D.E.M., Yusof, S.R., Begley, D.J., 2010. Structure and function of the blood-brain barrier. Neurobiol. Dis. 37, 13–25. http://dx.doi.org/10.1016/j.nbd.2009.07.030.

Adam, R., Greenberg, J.O., 1978. The mega cisterna magna. J. Neurosurg. 48, 190–192.

Aday, S., Cecchelli, R., Dehouck, M.P., Ferreira, L., 2016. Stem cell-based human blood-brain barrier models for drug discovery and delivery. Trends Biotechnol. 34, 382–393. http://dx.doi.org/10.1016/j.tibtech.2016.01.001.

Appel, S., Duke, E.S., Martinez, A.R., Khan, O.I., Dustin, I.M., Reeves-Tyer, P., Berl, M.B., Sato, S., Gaillard, W.D., Theodore, W.H., 2012. Cerebral blood flow and fMRI BOLD auditory language activation in temporal lobe epilepsy. Epilepsia 53, 631–638. http://dx.doi.org/10.1111/j.1528-1167.2012.03403.x.

Arrowsmith, J., Miller, P., 2013. Trial watch: phase II and phase III attrition rates 2011–2012. Nat. Rev. Drug Discov. 12, 569. http://dx.doi.org/10.1038/nrd4090.

Avdeef, A., Nielsen, P.E., Tsinman, O., 2004. PAMPA - a drug absorption in vitro model: 11. Matching the in vivo unstirred water layer thickness by individual-well stirring in microtitre plates. Eur. J. Pharm. Sci. 22, 365–374.

Baltes, S., Gastens, A.M., Fedrowitz, M., Potschka, H., Kaever, V., Löscher, W., 2007. Differences in the transport of the antiepileptic drugs phenytoin, levetiracetam and carbamazepine by human and mouse P-glycoprotein. Neuropharmacology 52, 333–346. http://dx.doi.org/10.1016/j.neuropharm.2006.07.038.

Bannwarth, B., Netter, P., Lapicque, F., Gillet, P., Péré, P., Boccard, E., Royer, R.J., Gaucher, A., 1992. Plasma and cerebrospinal fluid concentrations of paracetamol after a single intravenous dose of propacetamol. Br. J. Clin. Pharmacol. 34, 79–81. http://dx.doi.org/10.1111/j.1365-2125.1992.tb04112.x.

Beal, S., Sheiner, L., Boeckmann, A., Bauer, R., 2010. NONMEM User's Guides. Icon Development Solutions, Ellicott City.

Bednarczyk, J., Lukasiuk, K., 2011. Tight junctions in neurological diseases. Acta Neurobiol. Exp. (Wars) 71, 393–408.

Begley, D.J., Bradbury, M.W., Kreuter, J., 2000. The Blood-brain Barrier and Drug Delivery to the CNS. Marcel Dekker, Inc., New York. http://dx.doi.org/10.1016/S0168-3659(02)00422-4.

Bouw, R., Ederoth, P., Lundberg, J., Ungerstedt, U., Nordström, C.-H., Hammarlund-Udenaes, M., 2001. Increased blood-brain barrier permeability of morphine in a patient with severe brain lesions as determined by microdialysis case report. Acta Anaesthesiol. Scand. 45, 390–392.

Chen, H., Winiwarter, S., Fridén, M., Antonsson, M., Engkvist, O., 2011. In silico prediction of unbound brain-to-plasma concentration ratio using machine learning algorithms. J. Mol. Graph. Model. 29, 985–995.

Chodobski, A., Zink, B.J., Szmydynger-Chodobska, J., 2011. Blood-brain barrier pathophysiology in traumatic brain injury. Transl Stroke Res 2, 492–516. http://dx.doi.org/10.1007/s12975-011-0125-x.

Cornford, E.M., Hyman, S., 2005. Localization of brain endothelial luminal and abluminal transporters with immunogold electron microscopy. NeuroRx 2, 27–43.

Danhof, M., de Jongh, J., de Lange, E.C.M., Della Pasqua, O., Ploeger, B.A., Voskuyl, R.A., 2007. Mechanism-based pharmacokinetic-pharmacodynamic modeling: biophase distribution, receptor theory, and dynamical systems analysis. Annu. Rev. Pharmacol. Toxicol. 47, 357–400. http://dx.doi.org/10.1146/annurev.pharmtox.47.120505.105154.

de Lange, E.C.M., Danhof, M., de Boer, A.G., Breimer, D.D., 1994. Critical factors of intracerebral microdialysis as a technique to determine the pharmacokinetics of drugs in rat brain. Brain Res. 666, 1–8.

de Witte, W.E.A., Danhof, M., van der Graaf, P.H., de Lange, E.C.M., 2016. In vivo target residence time and kinetic selectivity: the association rate constant as determinant. Trends Pharmacol. Sci. 37, 831–842. http://dx.doi.org/10.1016/j.tips.2016.06.008.

Dean, M., 2004. Opioids in renal failure and dialysis patients. J. Pain Symptom Manag. 28, 497–504. http://dx.doi.org/10.1016/j.jpainsymman.2004.02.021.

Dekaban, A., Sadowsky, D., 1978. Changes in brain weights during the span of human life: relation of brain weights to body heights and body weights. Ann. Neurol. 4, 345–356. http://dx.doi.org/10.1002/ana.410040410.

Deo, A.K., Theil, F.-P., Nicolas, J.-M., 2013. Confounding parameters in preclinical assessment of blood-brain barrier permeation: an overview with emphasis on species differences and effect of disease states. Mol. Pharm. 10, 1581–1595. http://dx.doi.org/10.1021/mp300570z.

Dickens, D., Yusof, S.R., Abbott, N.J., Weksler, B., Romero, I.A., Couraud, P.O., Alfirevic, A., Pirmohamed, M., Owen, A., 2013. A multi-system approach assessing the interaction of anticonvulsants with P-gp. PLoS One 8. http://dx.doi.org/10.1371/journal.pone.0064854.

Dresel, S., Tatsch, K., Dahme, I., Mager, T., Scherer, J., Hahn, K., 1998. Iodine-123-iodobenzamide SPECT assessment of dopamine D2 receptor occupancy in risperidone treated schizophrenia patients. J. Nucl. Med. 39, 1138–1142.

Ederoth, P., Tunblad, K., Bouw, R., Lundberg, C.J., Ungerstedt, U., Nordstrom, C.H., Hammarlund-Udenaes, M., 2003. Blood-brain barrier transport of morphine in patients with severe brain trauma. Br. J. Clin. Pharmacol. 57, 427–435.

Fagerholm, U., 2007. The highly permeable blood-brain barrier: an evaluation of current opinions about brain uptake capacity. Drug Discov. Today 12, 1076–1082. http://dx.doi.org/10.1016/j.drudis.2007.10.005.

Feng, B., Mills, J.B., Davidson, R.E., Mireles, R.J., Janiszewski, J.S., Troutman, M.D., De Morais, S.M., 2008. In vitro P-glycoprotein assays to predict the in vivo interactions of P-glycoprotein with drugs in the central nervous system. Drug Metab. Dispos. 36, 268–275. http://dx.doi.org/10.1124/dmd.107.017434.

Fraser, D.G., Ludden, T.M., Evens, R.P., Sutherland, E.W., 1980. Displacement of phenytoin from plasma binding sites by salicylate. Clin. Pharmacol. Ther. 27, 165–169.

Friden, M., Gupta, A., Antonsson, M., Bredberg, U., Hammarlund-Udenaes, M., 2007. In vitro methods for estimating unbound drug concentrations in the brain interstitial and intracellular fluids. Drug Metab. Dispos. 35, 1711–1719. http://dx.doi.org/10.1124/dmd.107.015222.

Gazzard, B., Ford-Hutchinson, A., Smith, M., Williams, R., 1973. The binding of paracetamol to plasma proteins of man and pig. J. Pharm. Pharmacol. 25, 964–967.

Greve, M.W., Zink, B.J., 2009. Pathophysiology of traumatic brain injury. Mt Sinai J. Med. 76, 97–104. http://dx.doi.org/10.1002/msj.20104.

Groenendaal, D., Freijer, J., de Mik, D., Bouw, M.R., Danhof, M., de Lange, E.C.M., 2007. Population pharmacokinetic modelling of non-linear brain distribution of morphine: influence of active saturable influx and P-glycoprotein mediated efflux. Br. J. Pharmacol. 151, 701–712.

Grumetto, L., Russo, G., Barbato, F., 2016. Immobilized artificial membrane HPLC derived parameters vs PAMPA-BBB data in estimating in situ measured blood-brain barrier permeation of drugs. Mol. Pharm. 13, 2808–2816.

Ito, H., Inoue, K., Goto, R., Kinomura, S., Taki, Y., Okada, K., Sato, K., Sato, T., Kanno, I., Fukuda, H., 2006. Database of normal human cerebral blood flow measured by SPECT: I. Comparison between I-123-IMP, Tc-99m-HMPAO, and Tc-99m-ECD as referred with O-15 labeled water PET and voxel-based morphometry. Ann. Nucl. Med. 20, 131–138. http://dx.doi.org/10.1007/BF02985625.

Kalvass, J.C., Maurer, T.S., 2002. Influence of nonspecific brain and plasma binding on CNS exposure: implications for rational drug discovery. Biopharm. Drug Dispos. 23, 327–338. http://dx.doi.org/10.1002/bdd.325.

Kimelberg, H.K., 2004. Water homeostasis in the brain: basic concepts. Neuroscience 129, 851–860. http://dx.doi.org/10.1016/j.neuroscience.2004.07.033.

Kirvela, M., Lindgren, L., Seppala, T., Olkkola, K.T., 1996. The pharmacokinetics of oxycodone in uremic patients undergoing renal transplantation. J. Clin. Anesth. 8, 13–18. http://dx.doi.org/10.1016/0952-8180(95)00092-5.

Kitamura, A., Okura, T., Higuchi, K., Deguchi, Y., 2016. Cocktail-dosing microdialysis study to simultaneously assess delivery of multiple organic-cationic drugs to the brain. J. Pharm. Sci. 105, 935–940. http://dx.doi.org/10.1002/jps.24691.

Kokki, M., Välitalo, P., Kuusisto, M., Ranta, V.P., Raatikainen, K., Hautajärvi, H., Kokki, H., 2014. Central nervous system penetration of oxycodone after intravenous and epidural administration. Br. J. Anaesth. 112, 133–140. http://dx.doi.org/10.1093/bja/aet337.

Lazarowski, A., Czornyj, L., Lubienieki, F., Girardi, E., Vazquez, S., D'Giano, C., 2007. ABC transporters during epilepsy and mechanisms underlying multidrug resistance in refractory epilepsy. Epilepsia 48, 140–149.

Letrent, S.P., Polli, J.W., Humphreys, J.E., Pollack, G.M., Brouwer, K.R., Brouwer, K.L.R., 1999. P-glycoprotein-mediated transport of morphine in brain capillary endothelial

cells. Biochem. Pharmacol. 58, 951–957. http://dx.doi.org/10.1016/S0006-2952(99)00180-X.
Li, M., Yuan, H., Li, N., Song, G., Zheng, Y., Baratta, M., Hua, F., Thurston, A., Wang, J., Lai, Y., 2008. Identification of interspecies difference in efflux transporters of hepatocytes from dog, rat, monkey and human. Eur. J. Pharm. Sci. 35, 114–126. http://dx.doi.org/10.1016/j.ejps.2008.06.008.
Loryan, I., Sinha, V., Mackie, C., van Peer, A., Drinkenburg, W., Vermeulen, A., Morrison, D., Monshouwer, M., Heald, D., Hammarlund-Udenaes, M., 2014. Mechanistic understanding of brain drug disposition to optimize the selection of potential neurotherapeutics in drug discovery. Pharm. Res. 32, 2203–2219.
Loryan, I., Sinha, V., Mackie, C., van Peer, A., Drinkenburg, W.H., Vermeulen, A., Heald, D., Hammarlund-Udenaes, M., Wassvik, C.M., 2015. Molecular properties determining unbound intracellular and extracellular brain exposure of CNS drug candidates. Mol. Pharm. 12, 520–532.
Loryan, I., Melander, E., Svensson, M., Payan, M., König, F., Jansson, B., Hammarlund-Udenaes, M., 2016. In-depth neuropharmacokinetic analysis of antipsychotics based on a novel approach to estimate unbound target-site concentration in CNS regions: link to spatial receptor occupancy. Mol. Psychiatry 1–10.
Löscher, W., Potschka, H., 2002. Role of multidrug transporters in pharmacoresistance to antiepileptic drugs. J. Pharmacol. Exp. Ther. 301, 7–14. http://dx.doi.org/10.1124/jpet.301.1.7.
Luna-Tortós, C., Fedrowitz, M., Löscher, W., 2010. Evaluation of transport of common antiepileptic drugs by human multidrug resistance-associated proteins (MRP1, 2 and 5) that are overexpressed in pharmacoresistant epilepsy. Neuropharmacology 58, 1019–1032. http://dx.doi.org/10.1016/j.neuropharm.2010.01.007.
Mabondzo, A., Bottlaender, M., Guyot, A.C., Tsaouin, K., Deverre, J.R., Balimane, P.V., 2010. Validation of in vitro cell-based human blood-brain barrier model using clinical positron emission tomography radioligands to predict in vivo human brain penetration. Mol. Pharm. 7, 1805–1815. http://dx.doi.org/10.1021/mp1002366.
Mamo, D., Kapur, S., Shammi, C.M., Papatheodorou, G., Mann, S., Therrien, F., Remington, G., 2004. A PET study of dopamine D2 and serotonin 5-HT2 receptor occupancy in patients with schizophrenia treated with therapeutic doses of ziprasidone. Am. J. Psychiatry 161, 818–825. http://dx.doi.org/10.1176/appi.ajp.161.5.818.
Monteiro, J., Goraksha, S., 2017. 'ROSE concept' of fluid management: relevance in neuroanaesthesia and neurocritical care. J. Neuroanaesth. Crit. Care 4, 10. http://dx.doi.org/10.4103/2348-0548.197435.
Neuwelt, E., Abbott, N.J., Abrey, L., Banks, W.A., Blakley, B., Davis, T., Engelhardt, B., Grammas, P., Nedergaard, M., Nutt, J., Pardridge, W., Rosenberg, G.A., Smith, Q., Drewes, L.R., 2008. Strategies to advance translational research into brain barriers. Lancet Neurol. 7, 84–96.
Nguyen, T.-H.-T., Mouksassi, M.-S., Holford, N., Al-Huniti, N., Freedman, I., Hooker, A.C., John, J., Karlsson, M.O., Mould, D.R., Pérez Ruixo, J.J., Plan, E.L., Savic, R., van Hasselt, J.G.C., Weber, B., Zhou, C., Comets, E., Mentré, F., Model Evaluation Group of the International Society of PharmacometricsISoP Best Practice Committee, 2016. Model evaluation of continuous data pharmacometric models: metrics and graphics. In: CPT Pharmacometrics Syst. Pharmacol, pp. 1–20.
Ohtsuki, S., Ikeda, C., Uchida, Y., Sakamoto, Y., Miller, F., Glacial, F., Decleves, X., Scherrmann, J.M., Couraud, P.O., Kubo, Y., Tachikawa, M., Terasaki, T., 2013. Quantitative targeted absolute proteomic analysis of transporters, receptors and junction proteins for validation of human cerebral microvascular endothelial cell line hCMEC/D3 as a human blood-brain barrier model. Mol. Pharm. 10, 289–296. http://dx.doi.org/10.1021/mp3004308.
Okura, T., Hattori, A., Takano, Y., Sato, T., Hammarlund-udenaes, M., Terasaki, T., Deguchi, Y., 2008. Involvement of the pyrilamine transporter, a putative organic cation transporter, in blood-brain barrier transport of oxycodone. Drug Metab. Dispos. 36, 2005–2013. http://dx.doi.org/10.1124/dmd.108.022087.porter.
Pardridge, W.M., 2011. Drug transport in brain via the cerebrospinal fluid. Fluids Barriers CNS 8 (1), 7. http://dx.doi.org/10.1186/2045-8118-8-7.
Peterson, G.M., Mclean, S., Aldous, S., Witt, J.V.O.N., Millingen, K.S., 1982. Plasma protein binding of phenytoin in 100 epileptic patients. Br. J. Clin. Pharmacol. 14, 298–300.
Pop, V., Sorensen, D.W., Kamper, J.E., Ajao, D.O., Murphy, M.P., Head, E., Hartman, R.E., Badaut, J., 2013. Early brain injury alters the blood-brain barrier phenotype in parallel with b-amyloid and cognitive changes in adulthood. J. Cereb. Blood Flow Metab. 33, 205–214. http://dx.doi.org/10.1038/jcbfm.2012.154.
Potschka, H., Löscher, W., 2001a. In vivo evidence for P-glycoprotein-mediated transport of phenytoin at the blood-brain barrier of rats. Epilepsia 42, 1231–1240. http://dx.doi.org/10.1046/j.1528-1157.2001.01901.x.
Potschka, H., Löscher, W., 2001b. Multidrug resistance-associated protein is involved in the regulation of extracellular levels of phenytoin in the brain. Neuroreport 12, 2387–2389.
Rengachary, S.S., Ellenbogen, R.G., 2005. Principles of Neurosurgery. Elsevier Mosby, Edinburgh.
Robertson, E.G., 1949. Developmental defects of the cisterna magna and dura mater. J. Neurol. Neurosurg. Psychiatry 12, 39–51.
Sakka, L., Coll, G., Chazal, J., 2011. Anatomy and physiology of cerebrospinal fluid. Eur. Ann. Otorhinolaryngol. Head Neck Dis. 128, 309–316. http://dx.doi.org/10.1016/j.anorl.2011.03.002.
Shimomura, K., Okura, T., Kato, S., Couraud, P.-O., Schermann, J.-M., Terasaki, T., Deguchi, Y., 2013. Functional expression of a proton-coupled organic cation (H +/OC) antiporter in human brain capillary endothelial cell line hCMEC/D3, a human blood-brain barrier model. Fluids Barriers CNS 10, 8. http://dx.doi.org/10.1186/2045-8118-10-8.
Singla, N.K., Parulan, C., Samson, R., Hutchinson, J., Bushnell, R., Beja, E.G., Ang, R., Royal, M.A., 2012. Plasma and cerebrospinal fluid pharmacokinetic parameters after single-dose administration of intravenous, oral, or rectal acetaminophen. Pain Pract. 12, 523–532. http://dx.doi.org/10.1111/j.1533-2500.2012.00556.x.
Stange, K., Greitz, M., Ingvar, T., Hindmarsh, T., Sollevi, A., 1997. Global cerebral blood flow during infusion of adenosine in humans: assessment by magnetic resonance imaging and positron emission tomography. Acta Physiol. Scand. 160, 117–122.
Thorne, R.G., Hrabe, S., Nicholson, C., Robert, G., 2004. Diffusion of epidermal growth factor in rat brain extracellular space measured by integrative optical imaging. J. Neurophysiol. 92, 3471–3481.
Tunblad, K., Jonsson, E.N., Hammarlund-udenaes, M., 2003. Morphine blood-brain barrier transport is influenced by probenecid co-administration. 20, 618–623.
Wandel, C., Kim, R., Wood, M., Wood, A., 2002. Interaction of morphine, fentanyl, sufentanil, alfentanil, and loperamide with the efflux drug transporter P-glycoprotein. Anesthesiology 96, 913–920 (doi:00000542-200204000-00019 [pii]).
Westerhout, J., Danhof, M., de Lange, E.C.M., 2011. Preclinical prediction of human brain target site concentrations: considerations in extrapolating to the clinical setting. J. Pharm. Sci. 100, 3577–3593.
Westerhout, J., Ploeger, B., Smeets, J., Danhof, M., de Lange, E.C.M., 2012. Physiologically based pharmacokinetic modeling to investigate regional brain distribution kinetics in rats. AAPS J. 14, 543–553.
Westerhout, J., Smeets, J., Danhof, M., de Lange, E.C.M., 2013. The impact of P-gp functionality on non-steady state relationships between CSF and brain extracellular fluid. J. Pharmacokinet. Pharmacodyn. 40, 327–342.
Westerhout, J., van den Berg, D.-J., Hartman, R., Danhof, M., de Lange, E.C.M., 2014. Prediction of methotrexate CNS distribution in different species - influence of disease conditions. Eur. J. Pharm. Sci. 57, 11–24.
Wilder, B.J., Ramsay, R.E., Willmore, L.J., Feussner, G.F., Perchalski, R.J., Shumate, J.B., 1977. Efficacy of intravenous phenytoin in the treatment of status epilepticus: kinetics of central nervous system penetration. Ann. Neurol. 1, 511–518. http://dx.doi.org/10.1002/ana.410010602.
Wong, A.D., Ye, M., Levy, A.F., Rothstein, J.D., Bergles, D.E., Searson, P.C., 2013. The blood-brain barrier: an engineering perspective. Front. Neuroeng. 6, 1–22. http://dx.doi.org/10.3389/fneng.2013.00007.
Yamamoto, Y., Danhof, M., de Lange, E.C.M., 2017a. Microdialysis: the key to physiologically based model prediction of human CNS target site concentrations. AAPS J. 19, 891–909.
Yamamoto, Y., Välitalo, P.A., Huntjens, D.R., Proost, J.H., Vermeulen, A., Krauwinkel, W., Beukers, M.W., van den Berg, D.-J., Hartman, R., Wong, Y.C., Danhof, M., van Hasselt, J.G.C., de Lange, E.C.M., 2017b. Predicting drug concentration-time profiles in multiple relevant CNS compartments using a comprehensive physiologically based pharmacokinetic model. In: CPT Pharmacometrics Syst. Pharmacol.
Yamamoto, Y., Välitalo, P.A., van den Berg, D.-J., Hartman, R., van den Brink, W., Wong, Y.C., Huntjens, D.R., Proost, J.H., Vermeulen, A., Krauwinkel, W., Bakshi, S., Aranzana-Climent, V., Marchand, S., Dahyot-Fizelier, C., Couet, W., Danhof, M., van Hasselt, J.G.C., de Lange, E.C.M., 2017c. A generic multi-compartmental CNS distribution model structure for 9 drugs allows prediction of human brain target site concentrations. Pharm. Res. 34, 333–351.
Zhang, C., Kwan, P., Zuo, Z., Baum, L., 2010. In vitro concentration dependent transport of phenytoin and phenobarbital, but not ethosuximide, by human P-glycoprotein. Life Sci. 86, 899–905. http://dx.doi.org/10.1016/j.lfs.2010.04.008.